CONDENSED MATTER PHYSICS

Научная статья
Original article
DOI: https://doi.org/10.18721/JPM.16401

CURRENT–VOLTAGE CHARACTERISTICS OF $MAPBI_3$ PEROVSKITE FILMS FORMED BY THE SINGLE-STAGE SPIN-COAT METHOD

M. K. Ovezov[1]✉, *A. A. Ryabko*[1], *A. N. Aleshin*[1], *V. A. Moshnikov*[2], *V. M. Kondratyev*[3,4], *A. I. Maximov*[2]

[1] Ioffe Institute of RAS, St. Petersburg, Russia;

[2] St. Petersburg Electrotechnical University "LETI", St. Petersburg, Russia;

[3] Alferov University of RAS, St. Petersburg, Russia;

[4] Moscow Institute of Physics and Technology (National Research University), Moscow, Russia

✉strontiumx94@gmail.com

Abstract. In the paper, the properties of $MaPbI_3$ films made with or without a precipitant have been investigated. The samples had a planar geometry based on ceramic substrates with interdigitated gold electrodes and also based on glass substrates. The samples were irradiated with green light from an LED source, and a special setup was used to measure current–voltage (I–V) characteristics. The polycrystalline films exhibited high sensitivity (an increase in current by about 2 orders upon irradiation). The width of their optical band gap was the same regardless of the use of the precipitant but the maximum trap-filling voltages turned out to be very sensitive to such use. According to optical microscopy, the film microstructure was characterized by a growth of large long dendritic structures, i.e., the nucleation occurred in the solution mass during the films' making. This growth mechanism may be convenient for the use of $MaPbI_3$ films in photodetectors.

Keywords: organometallic perovskite, semiconducting polymer, transport mechanism, solar cell

Funding: The reported study was funded by Russian Science Foundation (Grant No. 23-42-10029; https://rscf.ru/en/project/23-42-10029/).

Citation: Ovezov M. K., Ryabko A. A., Aleshin A. N., Moshnikov V. A., Kondratyev V. M., Maximov A. I., Current – voltage characteristics of $MaPbI_3$ perovskite films formed by the single-stage spin-coat method, St. Petersburg State Polytechnical University Journal. Physics and Mathematics. 16 (4) (2023) 9–19. DOI: https://doi.org/10.18721/JPM.16401

УДК 538.91
DOI: https://doi.org/10.18721/JPM.16401

ВОЛЬТАМПЕРНЫЕ ХАРАКТЕРИСТИКИ ПЕРОВСКИТНЫХ ПЛЕНОК $MAPbI_3$, СФОРМИРОВАННЫХ ОДНОСТАДИЙНЫМ МЕТОДОМ ЦЕНТРИФУГИРОВАНИЯ

М. К. Овезов[1]✉, А. А. Рябко[1], А. Н. Алешин[1]
В. А. Мошников[2], В. М. Кондратьев[3,4], А. И. Максимов[2]

[1] Физико-технический институт им. А. Ф. Иоффе РАН, Санкт-Петербург, Россия;

[2] Санкт-Петербургский государственный электротехнический университет «ЛЭТИ» имени В. И. Ульянова (Ленина), Санкт-Петербург, Россия;

[3] Академический университет имени Ж. И. Алфёрова РАН, Санкт-Петербург, Россия;

[4] Московский физико-технический институт (Национальный исследовательский университет), Москва, Россия

✉strontiumx94@gmail.com

Аннотация. В работе исследованы свойства пленок $MaPbI_3$., изготовленных с применением осадителя либо без него. Образцы обладали планарной геометрией на основе керамических подложек со встречно-штыревыми золотыми электродами, а также на основе стеклянных подложек. Образцы облучали зеленым светом от светодиодного источника, а для измерения вольтамперных характеристик использовали специальную установку. Поликристаллические пленки продемонстрировали высокую фоточувствительность (увеличение тока примерно на 2 порядка при облучении). Ширина их оптической запрещенной зоны была одинаковой вне зависимости от использования осадителя, однако предельные напряжения заполнения ловушек оказались весьма чувствительными к такому использованию. По данным оптической микроскопии, для микроструктуры пленки характерно образование крупных дендритных структур, т.е. при ее изготовлении происходило зародышеобразование в толще раствора. Этот механизм может быть удобным для использования пленок $MaPbI_3$ в фотодетекторах.

Ключевые слова: металлорганический перовскит, полупроводящий полимер, механизм транспорта, солнечный элемент

Финансирование: Исследование проведено при финансовой поддержке Российского научного фонда (РНФ), грант № 23-42-10029; https://rscf.ru/en/project/23-42-10029/.

Ссылка для цитирования: Овезов М. К., Рябко А. А., Алешин А. Н., Мошников В. А., Кондратьев В. М., Максимов А. И. Вольтамперные характеристики перовскитных пленок $MaPbI_3$, сформированных одностадийным методом центрифугирования // Научно-технические ведомости СПбГПУ. Физико-математические науки. 2023. Т. 16. № 4. С. 9–19. DOI: https://doi.org/10.18721/JPM.16401

Introduction

Organometallic perovskites such as $(Fa)(Ma)MX_3$, where Fa is formamidinium $CH(NH_2)_2$, Ma is methylammonium CH_3NH_3, metal M = Pb, halogen X = Br or I, have been attracting increasing attention recently for applications in solar cells (SC) and photodetectors, X-ray detectors as well as memristor structures [1–3]. SC based on organometallic perovskites exhibit efficiency comparable to silicon solar cells (25.8%) [4]. In addition to organometallic perovskite films, films of inorganic perovskites $CsPbX_3$ are used for SE [5]. In this case, $CsPbX_3$ perovskite films are formed not only from a solution, but also from suspensions of

colloidal quantum dots, allowing to control the absorption spectrum of the SC by adjusting the size of the quantum dots [6–8]. Interest is also growing towards lead-free perovskite materials, primarily due to their low toxicity [9]. Even though SC based on lead-free perovskites exhibit lower efficiencies compared to lead-based ones (by about 6%), their stabilities are close to 2,000 hours of operation in a nitrogen atmosphere [10]. Finally, a promising direction is fabrication of tandem structures based on various SC combined with perovskite photovoltaic elements [11].

One of the best materials with a perovskite structure for creating SC is organometallic perovskite $CH_3NH_3PbI_3$ (referred to as $MaPbI_3$ from now on), also widely used to create photodetectors and X-ray detectors. Single-crtstal $MaPbI_3$ perovskite has been used for these detectors, demonstrating trap densities of the order of 10^{10} cm^{-3} and a carrier diffusion length exceeding 175 μm [12, 13]. Although single-crystal $MaPbI_3$ perovskite is also applicable for photovoltaic structures, it is economically impractical to use it for SC, as it is too difficult to produce a single crystal with a large diameter. Polycrystalline films are used to create SC, deposited from a solution by such methods as spray-coating, inkjet and screen printing, spin-coating and others [14].

As a rule, polycrystalline layers of $MaPbI_3$ are deposited by spin-coating in two steps if PbI_2 and CH_3NH_3I solutions are deposited separately, or in one step if $CH_3NH_3PbI_3$ solution is deposited. Studies producing the materials discovered that the two-step method allows to obtain more homogeneous films, but it is more technologically complex, while films made by two different methods yield comparable characteristics, some (for example, grain size) even better for films prepared by the one-step method [15, 16].

Analyzing the available data, we opted for the one-step method. A precipitator is often used for depositing the film, allowing to considerably improve the quality of the film [17–19]. Many reagents can be used as precipitators, but ethyl acetate (EA) stands out in that it allows to achieve a sufficiently high efficiency of the photosensitive layer (up to 19.53%). In addition, this layer can preserve up to 84.8% of the initial efficiency in an SC operating in an open air environment for a long time (over 1900 hours) [20]. Additionally, ethyl acetate has low cost and low toxicity, offering greater prospects for commercial applications.

In this paper, we considered the influence of the technology for manufacturing the MaPbI perovskite film on its current–voltage characteristics in planar structures was investigated; ethyl acetate was deposited in a one-step procedure in this case.

Materials and methods

Powders of $MaPbI_3$ organometallic perovskites purchased from Xi'an Polymer Light Technology Corp. (China) were used to prepare the samples. The films were applied by spin-coating from a solution of dimethylformamide and dimethyl sulfoxide (4:1 volume ratio) with a $MaPbI_3$ mass concentration of 300 mg/ml with subsequent annealing at a temperature of 110 °C for 10 minutes. The spin-coating rate was 3000 rpm (for 30 s) with pre-centrifugation at 1000 rpm (10 s). The samples were obtained by two techniques: using ethyl acetate as a precipitator and without it. The precipitator was introduced at the acceleration stage of spin coating.

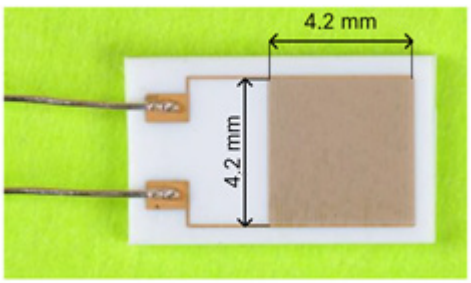

Fig. 1. Photo of ceramic substrate with interdigitated NiCr/Ni/Au electrodes (sensor platform, Tesla Blatná)
The size of the region with these electrodes is 4.2 × 4.2 mm

The current–voltage characteristics were measured by depositing the perovskite films on ceramic substrates with interdigitated gold electrodes (sensor platform from Tesla Blatná, Czech Republic). The thickness of the electrodes and the distance between them was 25 μm (Fig. 1).

The sample morphology was studied by optical and scanning electron microscopy, also depositing layers of $MaPbI_3$ perovskite film on silicon substrates. To determine the band gap width by processing the optical absorption spectra, such layers were deposited on glass substrates with ITO coating. The latter is a solution consisting of indium, oxygen and tin, i.e., indium oxide In_2O_3 and tin oxide Sn_2O_3.

The current–voltage (I–V) characteristics of the samples were measured with a Keithley 6487 picoammeter (USA) in the dark and under illumination with an LED source at a wavelength of 535 nm. The absorption spectra were measured with a PE-5400UF spectrophotometer (Russia). The microstructure of the objects was studied with a POLAM-312 polarizing microscope (Russia). The morphology of the coatings was also studied with a Zeiss Supra 25 scanning electron microscope (Germany).

Results and discussion

The samples of thin polycrystalline $MaPbI_3$ films obtained in this study exhibit a characteristic optical absorption spectrum (curve *1* in Fig. 2,*a*). The optical band gap of the samples was determined as a Tauc plot, $(\alpha h\nu)^{1/r}$ versus $h\nu$, by extrapolating the linear section to the abscissa axis, where the value of r expresses the type of dependence of the semiconductor's absorption coefficient on the irradiation wavelength (greater than the semiconductor's absorption edge). Since $MaPbI_3$ is a direct band gap semiconductor, the absorption coefficient is described by the root dependence on the wavelength ($r = 1/2$).

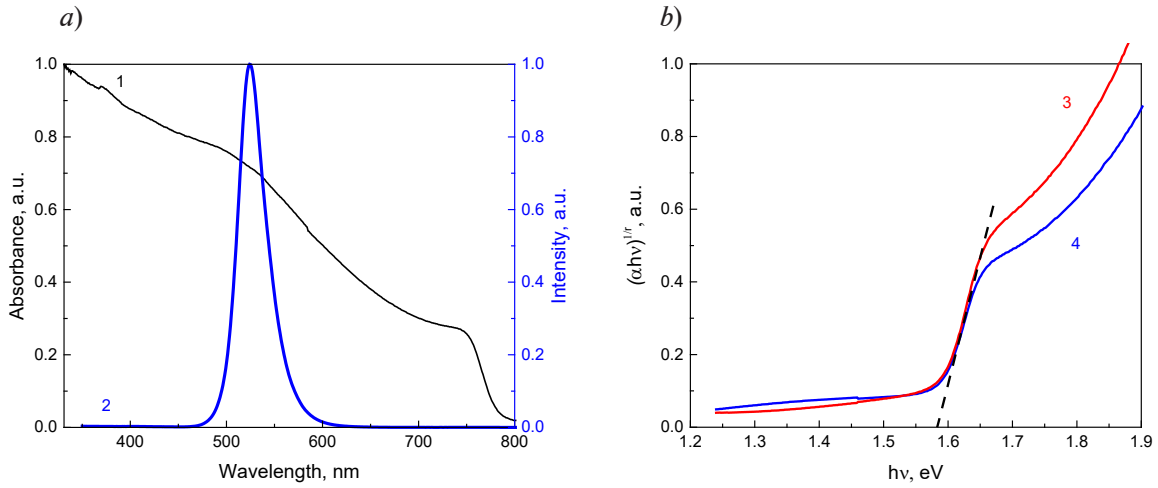

Fig. 2. Analysis of $MaPbI_3$ layers (curve *1* in Fig. 2,*a*, curves *3*, *4* in Fig. 2,*b*), and LED source (curve *2* in Fig. 2,*a*):
typical optical absorption spectrum *1*; optical absorption spectra *3*, *4* as Tauc plots for determining the optical band gap; dependences are shown for samples prepared with a precipitator (*3*) and without it (*4*); *2* is the electroluminescence spectrum of a green LED used to record the photo response of samples

According to the results obtained, the optical band gap E_g of the manufactured films was $E_g \approx 1.58$ eV, and this value did not depend on whether a precipitator was used; it is characteristic for polycrystalline $MaPbI_3$ films.

The results of I–V measurements in the dark and under illumination are shown in Figs. 3 and 4. The samples exposed to irradiation with green light leads exhibit a change in the current by about two orders of magnitude, while using a precipitator does not have a noticeable effect. The current–voltage characteristics in the dark exhibit hysteresis, which is associated with migration of ions (primarily I^-), as well as the space-charge limited current (SCLC) [20]. The influence of the technology by which the samples were prepared is also observed: the maximum trap-filling voltages V_{TFL} differ for samples obtained with and without the precipitator.

We also found a slight increase in V_{TFL} after the samples were irradiated with light (a green LED was used), pointing to an increase in trap concentration during exposure.

It was found in [20] that such irradiation can significantly accelerate or induce ion migration, and such migration is observed over a wide temperature range. A five-fold decrease in the activation energy of ion migration is also reported (from 0.82 to 0.15 eV with an increase in the irradiation intensity from 0 to 20 MW/cm^2) [21].

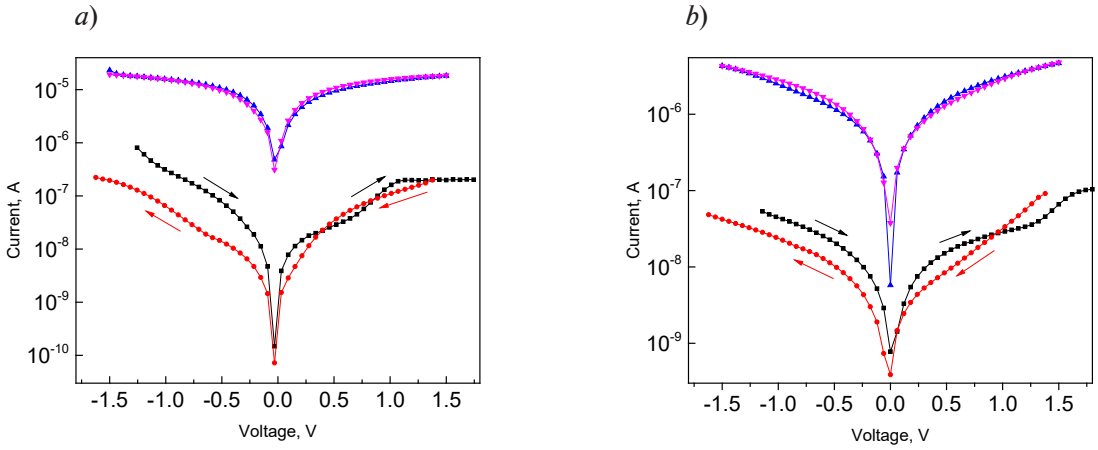

Fig. 3. $I-V$ curves of the samples prepared without precipitator (*a*) and with it (*b*) in the dark (lower curves) and under irradiation with green light (upper curves)
The arrows indicate the variation modes of the voltages applied to the samples

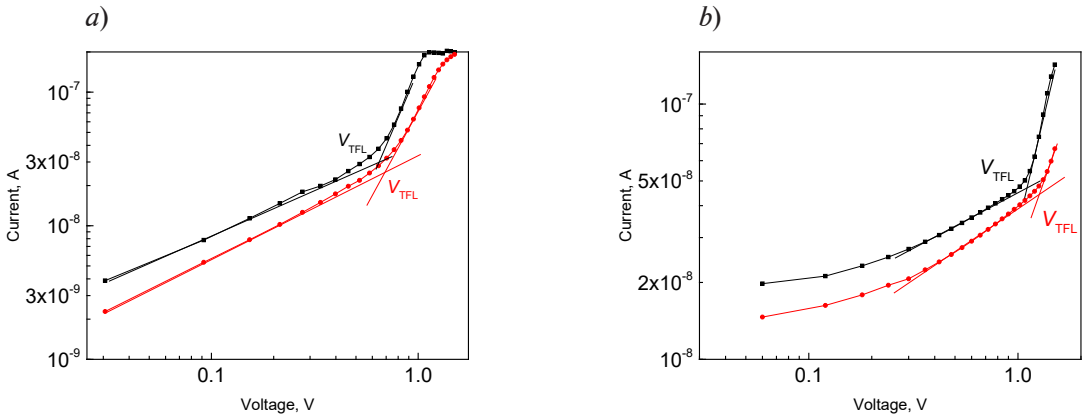

Fig. 4. Fragments of $I-V$ curves of the samples prepared without precipitator (*a*) and with it (*b*) in the dark, obtained before (black curves) and after (red curves) irradiation with light.
A difference in V_{TFL} values is observed.

The maximum trap-filling voltage V_{TFL} is directly proportional to their concentration:

$$V_{TFL} = \frac{eN_t L^2}{2\varepsilon\varepsilon_0}, \tag{1}$$

where e is the electron charge, N_t is the trap concentration, L is the distance between the electrodes (25 μm for our case), ε is the permittivity of the material (ε = 32 for $MaPbI_3$), ε_0 is the dielectric constant [18].

The concentration of traps can be calculated from this using the formula

$$N_t = \frac{2\varepsilon\varepsilon_0 V_{TFL}}{eL^2}. \tag{2}$$

N_t values equal to 3.68, 3.81, 6.09 and 7.01 (10^{14} cm^{-3}), respectively, were obtained for a voltage V_{TFL} of approximately 0.65–0.70 V for a sample without precipitator and about 1.13 – 1.30 V for a sample with precipitator.

The values of V_{TFL} and, consequently, the trap concentrations turned out to be lower for the sample obtained without precipitator, which is inconsistent with the literature data [16, 22].

The results obtained by scanning electron microscopy (Fig. 5, *c*, *d*) indicate that using the precipitator (ethyl acetate) under these conditions produces an increase in the size of film crystallites, compared with the film prepared without the precipitator. There are also pores in the films due to the conditions of solvent evaporation. The optical microscopy data (Fig. 5,*a*) for the sample obtained with a precipitator indicate that some substrate regions are not covered by the perovskite film, however, the regions covered by the $MaPbI_3$ film are homogeneous. On the other hand, not only heterogeneous nucleation is observed for the sample obtained without precipitator at the interface with the substrate, but also growth of large elongated (~50 μm) dendritic structures (Fig. 5,*d*).

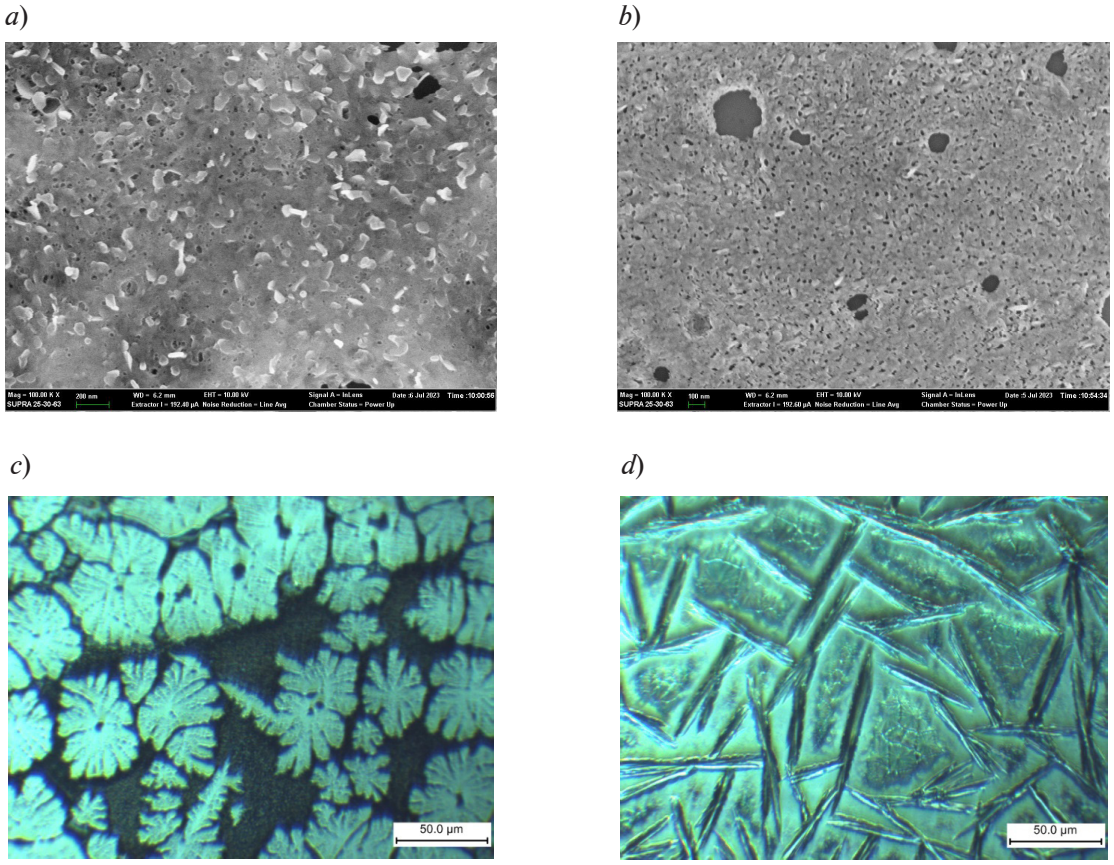

Fig. 5. Micrographs of $MaPbI_3$ layers for samples prepared with precipitator (*a*,*c*) and without it (*b*,*d*) obtained by optical (*a*, *b*) and scanning electron (*c*, *d*) microscopy

Evidently, as the solvent evaporates from the $MaPbI_3$ solution under heating, this can lead to an increase in the solute concentration near the surface. Moreover, the temperature gradient from the substrate surface to the film surface leads to a decrease in the solubility of the $MaPbI_3$ film in the near-surface region.

Thus, the conditions for nucleation are fulfilled near the surface of the solution film, with subsequent growth of dendritic structures. Nucleation at the phase boundary is energetically favorable, inducing growth of polycrystalline film directly on the surface of the substrate (Fig. 5,*b*). Consequently, the precipitator leads to an increase in the size of the film crystallites formed at the phase boundary, however, the conditions of film growth without precipitator lead to growth of elongated $MaPbI_3$ structures of a larger scale.

Although the conditions for film growth are different if polished surfaces of silicon substrates and ceramic substrates are used, due to the different concentrations of nucleation sites on the substrate surface and hydrophobicity, we assume that the character of film formation

should be similar. Thus, the film consisting of elongated structures has a lower concentration of grain boundaries, which leads to a decrease in the trap concentration and the voltage V_{TFL}. Although this growth mechanism hinder the application of polycrystalline films in photovoltaic structures, it may be convenient for using $MaPbI_3$ films in photodetectors. On the other hand, using a precipitator is preferable from the standpoint of morphology of such a film for creating photovoltaic structures.

Conclusions

Films of organometallic perovskite $MaPbI_3$ produced for the study exhibit a high response to visible-light irradiation (with a green LED) as well as to the characteristic mode of space charge limited current. The dark current–voltage (I–V) characteristics exhibit hysteresis due to ion migration.

We found that $MaPbI_3$ films prepared by the described procedure without the precipitator contain large dendritic structures providing a decrease in the maximum trap-filling voltage We believe that films with such morphology can be successfully used as photodetectors.

REFERENCES

1. **Sakhatskyi K., Tьredi B., Matt G. J., et al.,** Stable perovskite single-crystal X-ray imaging detectors with single-photon sensitivity, Nat. Photon. 17 (June) (2023) 510–517.

2. **Wang H., Sun Y., Chen J., et al.,** Review of perovskite-based photodetectors and their applications, Nanomater. 12 (24) (2022) 4390.

3. **Nenashev G. V., Aleshin A. N., Shcherbakov I. P., Petrov V. N.,** Effect of temperature variations on the behavior of a two-terminal organic-inorganic halide perovskite rewritable memristor for neuromorphic operations, Solid State Commun. 348–349 (1 June) (2022) 114768.

4. **Roy P., Ghosh A., Barclay F., et al.,** Perovskite solar cells: A review of the recent advances, Coat. 12 (8) (2022) 1089.

5. **Wang J., Zhang J., Zhou Y., et al.,** Highly efficient all-inorganic perovskite solar cells with suppressed non-radiative recombination by a Lewis base, Nat. Commun. 11 (Jan) (2020) 177.

6. **Sadhu A. S., Huang Y.-M., Chen L.-Y., et al.,** Recent advances in colloidal quantum dots or perovskite quantum dots as a luminescent downshifting layer embedded on solar cells, Nanomater. 12 (6) (2022) 985.

7. **Srivastava A. K., Zhang W., Schneider J., et al.,** Luminescent down-conversion semiconductor quantum dots and aligned quantum rods for liquid crystal displays, Adv. Sci. 6 (22) (2019) 1901345.

8. **Aleksandrova O. A., Galieva D. M., Drobinceva A. O., et al.,** Nanochastitsy, nanosistemy i ikh primeneniye. Ch.1. Kolloidnyye kvantovyye tochki [Nanoparticles, nano systems and their application. Part 1. Colloidal quantum dots], Aeterna Publishing, Ufa, 2015 (in Russian).

9. **Shi Z. J., Guo J., Chen Y. H., et al.,** Lead-free organic-inorganic hybrid perovskites for photovoltaic applications: Recent advances and perspectives, Adv. Mater. 29 (16, 3 Febr.) (2017) 1605005.

10. **Gao W., Ran C., Li J., et al.,** Robust stability of efficient lead-free formamidinium tin iodide perovskite solar cells realized by structural regulation, J. Phys. Chem. Lett. 9 (24) (2018) 6999–7006.

11. **Li H., Zhang W.,** Perovskite tandem solar cells: From fundamentals to commercial deployment, Chem. Rev. 120 (18) (2020) 9835–9950.

12. **Rong Sh.-Sh., Faheem M. B., Li Y.-B.,** Perovskite single crystals: Synthesis, properties, and applications, J. Electron. Sci. Technol. 19 (2) (2021) 100081.

13. **Lian Zh., Yan Q., Gao T., et al.,** Perovskite $CH_3NH_3PbI_3(Cl)$ single crystals: Rapid solution growth, unparalleled crystalline quality, and low trap density toward 10^8 cm^{-3}, J. Am. Chem. Soc. 138 (30) (2016) 9409–9412.

14. **Zhang Y., Zhang H., Zhang X., et al.,** Major impediment to highly efficient, stable and low-cost perovskite solar cells, Metals. 8 (11) (2018) 964.

15. **Xiao M., Huang F., Huang W., et al.,** A fast deposition-crystallization procedure for highly efficient lead iodide perovskite thin-film solar cells, Angew. Chem. Int. Edit. 53 (37) (2014) 9898–9903.

16. **Ahmed D. S., Mohammed B. K., Mohammed M. K. A.,** Long-term stable and hysteresis-free planar perovskite solar cells using green antisolvent strategy, J. Mater. Sci. 56 (27) (2021) 15205–15214.

17. **Shaikh J. S., Shaikh N. S., Sheikh A. D., et al.,** Perovskite solar cells: In pursuit of efficiency and stability, Mater. Design. 136 (15 Dec) (2017) 54–80.

18. **Li D., Shi J., Xu Y., et al.,** Inorganic-organic halide perovskites for new photovoltaic technology, Natl. Sci. Rev. 5 (4) (2018) 559–576.

19. **Zhang W., Li Y., Liu X., et al.,** Ethyl acetate green antisolvent process for high-performance planar low-temperature SnO_2-based perovskite solar cells made in ambient air, Chem. Eng. J. 379 (1 Jan) (2020) 122298.

20. **Zhang P., Gu N., Song L., et al.,** The disappearing additive: introducing volatile ethyl acetate into a perovskite precursor for fabricating high efficiency stable devices in open air, Nanoscale. 14 (13) (2020) 5204–5213.

21. **Khan R., Ighodalo K.O., Z. Xiao Z.,** Ion migration in metal halide perovskites solar cells, soft-matter thin film solar cells: Physical processes and device simulation, AIP Publishing LLC, Melville, New York, 2020, p. 1-283.

22. **Zhao Y.-C., Zhou W.-K., Zhou X., et al.,** Quantification of light-enhanced ionic transport in lead iodide perovskite thin films and its solar cell applications, Light Sci. Appl. 6 (5, 5 May) (2017) e16243.

СПИСОК ЛИТЕРАТУРЫ

1. **Sakhatskyi K., Tьredi B., Matt G. J., et al.** Stable perovskite single-crystal X-ray imaging detectors with single-photon sensitivity // Natural Photonics. 2023. Vol. 17. June. Pp. 510–517.

2. **Wang H., Sun Y., Chen J., Wang F., Han R., Zhang C., Kong J., Li L., Yang J. A.** Review of perovskite-based photodetectors and their applications // Nanomaterials. 2022. Vol. 12. No. 24. P. 4390.

3. **Nenashev G. V., Aleshin A. N., Shcherbakov I. P., Petrov V. N.** Effect of temperature variations on the behavior of a two-terminal organic-inorganic halide perovskite rewritable memristor for neuromorphic operations // Solid State Communications. 2022. Vol. 348–349. 1 June. P. 114768.

4. **Roy P., Ghosh A., Barclay F., Khare A., Cuce E.** Perovskite solar cells: A review of the recent advances // Coatings. 2022. Vol. 12. No. 8. P. 1089.

5. **Wang J., Zhang J., Zhou Y., Liu H., Xue Q., Li X., Jen A. K.** Highly efficient all-inorganic perovskite solar cells with suppressed non-radiative recombination by a Lewis base // Nature Communications. 2020. Vol. 11. January. P. 177.

6. **Sadhu A. S., Huang Y.-M., Chen L.-Y., Kuo H.-C., Lin C.-C.** Recent advances in colloidal quantum dots or perovskite quantum dots as a luminescent downshifting layer embedded on solar cells // Nanomaterials. 2022. Vol. 12. No. 6. P. 985.

7. **Srivastava A. K., Zhang W., Schneider J., Halpert J. E., Rogach A. L.** Luminescent down-conversion semiconductor quantum dots and aligned quantum rods for liquid crystal displays // Advanced Science. 2019. Vol. 6. No. 22. P. 1901345.

8. **Александрова О. А., Галиева Д. М., Дробинцева А. О. и др.** Наночастицы, наносистемы и их применение. Ч. 1. Коллоидные квантовые точки. Под ред. В. А. Мошникова, О. А. Александровой. Уфа: Аэтерна, 2015. 236 с.

9. **Shi Z. J., Guo J., Chen Y. H., Li Q., Pan Y. F., Zhang H. J., Xia Y. D., Huang W.** Lead-free organic-inorganic hybrid perovskites for photovoltaic applications: Recent advances and perspectives // Advanced Materials. 2017. Vol. 29. No. 16. 3 February. P. 1605005.

10. **Gao W., Ran C., Li J., Dong H., Jiao B., Zhang L., Lan X., Hou X., Wu Z.** Robust stability of efficient lead-free formamidinium tin iodide perovskite solar cells realized by structural regulation // The Journal of Physical Chemistry Letters. 2018. Vol. 9. No. 24. Pp. 6999–7006.

11. **Li H., Zhang W.** Perovskite tandem solar cells: From fundamentals to commercial deployment // Chemical Reviews. 2020. Vol. 120. No. 18. Pp. 9835–9950.

12. **Rong Sh.-Sh., Faheem M. B., Li Y.-B.** Perovskite single crystals: Synthesis, properties, and applications. // Journal of Electronic Science and Technology. 2021. Vol. 19. No. 2. P. 100081.

13. **Lian Zh., Yan Q., Gao T., Ding J., Lv Q., Ning Ch., Li Q., Sun J.-L.** Perovskite $CH_3NH_3PbI_3(Cl)$ single crystals: Rapid solution growth, unparalleled crystalline quality, and low trap density toward 10^8 cm^{-3}// Journal of the American Chemical Society. 2016. Vol. 138. No. 30. Pp. 9409–9412.

14. **Zhang Y., Zhang H., Zhang X., Wei L., Zhang B., Sun Y., Hai G., Li Y.** Major impediment to highly efficient, stable and low-cost perovskite solar cells // Metals. 2018. Vol. 8. No. 11. P. 964.

15. **Xiao M., Huang F., Huang W., Dkhissi Y., Zhu Y., Etheridge J., Gray-Weale A., Bach U., Cheng Y., Spiccia L.** A fast deposition-crystallization procedure for highly efficient lead iodide perovskite thin-film solar cells // Angewandte Chemie International Edition. 2014. Vol. 53. No. 37. Pp. 9898–9903.

16. **Ahmed D. S., Mohammed B. K., Mohammed M. K. A.** Long-term stable and hysteresis-free planar perovskite solar cells using green antisolvent strategy // Journal of Materials Science. 2021. Vol. 56. No. 27. Pp. 15205–15214.

17. **Shaikh J. S., Shaikh N. S., Sheikh A. D., Mali S. S., Kale A. J., Kanjanaboos P., Hong C. K., Kim J. H., Patil P. S.** Perovskite solar cells: In pursuit of efficiency and stability // Materials & Design. 2017. Vol. 136. 15 December. Pp. 54–80.

18. **Li D., Shi J., Xu Y., Luo Y., Wu H., Meng Q.** Inorganic-organic halide perovskites for new photovoltaic technology // National Science Review. 2018. Vol. 5. No. 4. Pp. 559–576.

19. **Zhang W., Li Y., Liu X., Tang D., Li X., Yuan X.** Ethyl acetate green antisolvent process for high-performance planar low-temperature SnO_2-based perovskite solar cells made in ambient air // Chemical Engineering Journal. 2020. Vol. 379. 1 January. P. 122298.

20. **Zhang P., Gu N., Song L., Chen X., Du P., Zha L., Chen W.-Hs., Xiong J.** The disappearing additive: introducing volatile ethyl acetate into a perovskite precursor for fabricating high efficiency stable devices in open air // Nanoscale. 2022. Vol. 14. No. 13. Pp. 5204–5213.

21. **Khan R., Ighodalo K.O., Z. Xiao Z.** Ion migration in metal halide perovskites solar cells, soft-matter thin film solar cells: Physical processes and device simulation. Melville, New York: AIP Publishing LLC, 2020. p. 1-283

22. **Zhao Y.-C., Zhou W.-K., Zhou X., Liu K.-H., Yu D.-P., Zhao K.** Quantification of light-enhanced ionic transport in lead iodide perovskite thin films and its solar cell applications // Light: Science & Applications. 2017. Vol. 6. No. 5. 5 May. P. e16243.

THE AUTHORS

OVEZOV Maksat K.
Ioffe Institute, RAS
26 Polytekhnicheskaya St., St. Petersburg, 194021, Russia
strontiumx94@gmail.com
ORCID: 0009-0009-6273-1478

RYABKO Andrey A.
Ioffe Institute, RAS
26 Polytekhnicheskaya St., St. Petersburg, 194021, Russia
a.a.ryabko93@yandex.ru
ORCID: 0000-0001-9626-7612

ALESHIN Andrey N.
Ioffe Institute, RAS
26 Polytekhnicheskaya St., St. Petersburg, 194021, Russia
aleshin.transport@mail.ioffe.ru
ORCID: 0000-0001-5449-4446

MOSHNIKOV Vyacheslav A.
St. Petersburg Electrotechnical University "LETI"
5 Professor Popov St., St. Petersburg, 197376, Russia
vamoshnirov@mail.ru
ORCID: 0000-0001-6500-5492

KONDRATYEV Valeriy M.
Alferov University, RAS
Moscow Institute of Physics and Technology (National Research University)
8/3 Khlopin St., St. Petersburg, 194021, Russia
kvm_96@mail.ru
ORCID: 0000-0002-3469-5897

MAXIMOV Alexander I.
St. Petersburg Electrotechnical University "LETI"
5 Professor Popov St., St. Petersburg, 197376, Russia
aimaximov@mail.ru
ORCID: 0000-0003-0195-8870

СВЕДЕНИЯ ОБ АВТОРАХ

ОВЕЗОВ Максат Кемалович – *младший научный сотрудник лаборатории неравновесных процессов в полупроводниках Физико-технического института имени А. Ф. Иоффе Российской академии наук.*
194021, *Россия*, г. Санкт-Петербург, Политехническая ул., 26
strontiumx94@gmail.com
ORCID: 0009-0009-6273-1478

РЯБКО Андрей Андреевич – *кандидат технических наук, младший научный сотрудник лаборатории неравновесных процессов в полупроводниках Физико-технического института имени А. Ф. Иоффе Российской академии наук.*
194021, *Россия*, г. Санкт-Петербург, Политехническая ул., 26
a.a.ryabko93@yandex.ru
ORCID: 0000-0001-9626-7612

АЛЕШИН Андрей Николаевич – *доктор физико-математических. наук, заведующий лабораторией неравновесных процессов в полупроводниках Физико-технического института имени А. Ф. Иоффе Российской академии наук.*
194021, *Россия*, *г.* Санкт-Петербург, Политехническая ул., 26
aleshin.transport@mail.ioffe.ru
ORCID: 0000-0001-5449-4446

МОШНИКОВ Вячеслав Алексеевич – *доктор физико-математических наук, профессор кафедры микро- и наноэлектроники Санкт-Петербургского государственного электротехнического университета «ЛЭТИ» имени В. И. Ульянова (Ленина).*
197376, *Россия*, г. Санкт Петербург, ул. Проф. Попова, 5
vamoshnirov@mail.ru
ORCID: 0000-0001-6500-5492

КОНДРАТЬЕВ Валерий Михайлович – *аспирант Академического университета имени Ж. И. Алфёрова Российской академии наук, г. Санкт-Петербург; младший научный сотрудник Московского физико-технического института (Национального исследовательского университета).*
194021, *Россия*, г. Санкт-Петербург, ул. Хлопина, 8/3
kvm_96@mail.ru
ORCID: 0000-0002-3469-5897

МАКСИМОВ Александр Иванович – *кандидат физико-математических наук, доцент кафедры микро- и наноэлектроники Санкт-Петербургского государственного электротехнического университета «ЛЭТИ» имени В. И. Ульянова (Ленина).*
197376, *Россия*, г. Санкт Петербург, ул. Проф. Попова, 5
aimaximov@mail.ru
ORCID: 0000-0003-0195-8870

Received 14.09.2023. Approved after reviewing 20.10.2023. Accepted 20.10.2023.
Статья поступила в редакцию 14.09.2023. Одобрена после рецензирования 20.10.2023. Принята 20.10.2023.